

Research article

Investigation of paleochannel identification using radar and optical images on placer deposits in Bangka Barat Regency, Indonesia

Riset Geologi dan Pertambangan
Indonesian Journal of Geology
and Mining
Vol.32, No 2 pages 71–81

doi:

10.14203/jrisetgeotam2022.v32.1183

Keywords:

paleochannel,
remote sensing,
radar,
West Bangka

Corresponding author:

Asep Saepuloh
Email Address: saepuloh@itb.ac.id

Article history

Received: 14 September 2021

Revision: 11 April 2022

Accepted: 02 July 2022

©2022 BRIN

This is an open access article under
the CC BY-NC-SA license
(<http://creativecommons.org/licenses/by-nc-sa/4.0/>).



Ruri Pitaloka¹, Asep Saepuloh², Slamet Sugiharto³

¹ PT. Antam Tbk., Jl. TB Simatupang 1, South Jakarta, Indonesia

² Geological Engineering Study Program, Faculty of Earth Sciences and Technology, Bandung Institute of Technology, Jl. Ganesha No.10, Bandung, West Java, Indonesia.

³ PT. Timah Tbk., Jl. Jenderal Sudirman 51 Pangkal Pinang, Bangka, Indonesia.

ABSTRACT This article is about a visual investigation of paleochannel identification using ALOS 2 PALSAR 2 (Advanced Land Observing Satellite 2 Phased Array type L-band Synthetic Aperture Radar 2) radar satellite image. The radar image has a higher layer-penetration ability than the optical image so that the characteristics of near-surface materials are possible to be detected, including the morphology of the abandoned river stream. The purpose of ancient channels investigation is to localize potential areas of tin placer deposits, including rare earth elements as associated minerals. This investigation was aided by LANDSAT 8 optical image and National Digital Elevation Model (DEMNAS) data. Visual identification has been performed based on the shape, color, pattern, texture, and position against other morphologies in the image. The criteria for paleochannels are the channels detected using ALOS 2 PALSAR 2 image but not in LANDSAT 8 optical image and DEMNAS data. Based on these criteria, eleven traces of paleochannels have been well identified. Their occurrences are generally associated with meanders, open areas, and near the coast. The detected paleochannels are generally purple to dark in the color composite of the ALOS 2 PALSAR 2 image. These detected rivers are in pink to purplish-green zones and have a random appearance.

INTRODUCTION

Bangka Island is a part of the Southeast Asia Tin Belt (Cobbing et al., 1986) extends from the Malay Peninsula, Riau Islands, Singkep, Bangka, and Belitung. Generally, it has been subjected to intensive erosion over a long period, producing the formation of many paleochannels. Many studies related to paleochannel in Bangka offshore have been published, while the publication of paleochannel research on mainland Bangka is limited.

Application of remote sensing technology to identify paleochannel, specifically paleochannel in land areas with tropical rainforest climates, is uncommon due to dense vegetation, high weathering and humidity levels. Remote sensing methods are much more often applied in paleochannel identification found in desert areas (Paillou et al., 2012). Meanwhile, the common methods for paleochannel identification in tropical climates are geophysical surveys (seismic surveys) for offshore and resistivity

or GPR (Ground Penetrating Radar) for land areas (Zainal et al., 2017; Bennett et al., 2006). However, in 2020, the identification of paleochannel in parts of China's plains was successfully carried out by processing DEM (Digital Elevation Model) combined with discoveries of historical objects locations and other additional data which not further explained (Zhang et al., 2020). Paleochannels can be well visualized from the results of the DEM logarithmic transformation and further processing. This method is effectively used to detect river migration in a vast mainland area (the case study is about 1,000,000 km²) and subtropical - dry climate.

In contrast to mainland China, which is very large and accompanied by many locations for discovering historical objects and has a subtropical to dry climate (Kottek et al., 2006), Bangka Island is only 11,964 km², has a tropical rainforest climate, and is surrounded by the waters. The morphology is dominated by denudational hills. Most of the area is covered by vegetation in the form of oil palm plantations, settlements, coastal areas, and open areas resulting from tin mining activities. The observation area is a small part of Bangka Island, located in the western part of the West Bangka Regency (Figure 1). It has a stratigraphic sequence from oldest to youngest Pemali Complex (Permian), Diabas Sabung (Permian), Klabat Granite (Late Triassic), Tanjunggenting Formation (Triassic), Ranggalam Formation (Miocene-Pliocene), and Alluvium Deposits (Quaternary) (Mangga & Djamal, 1994).

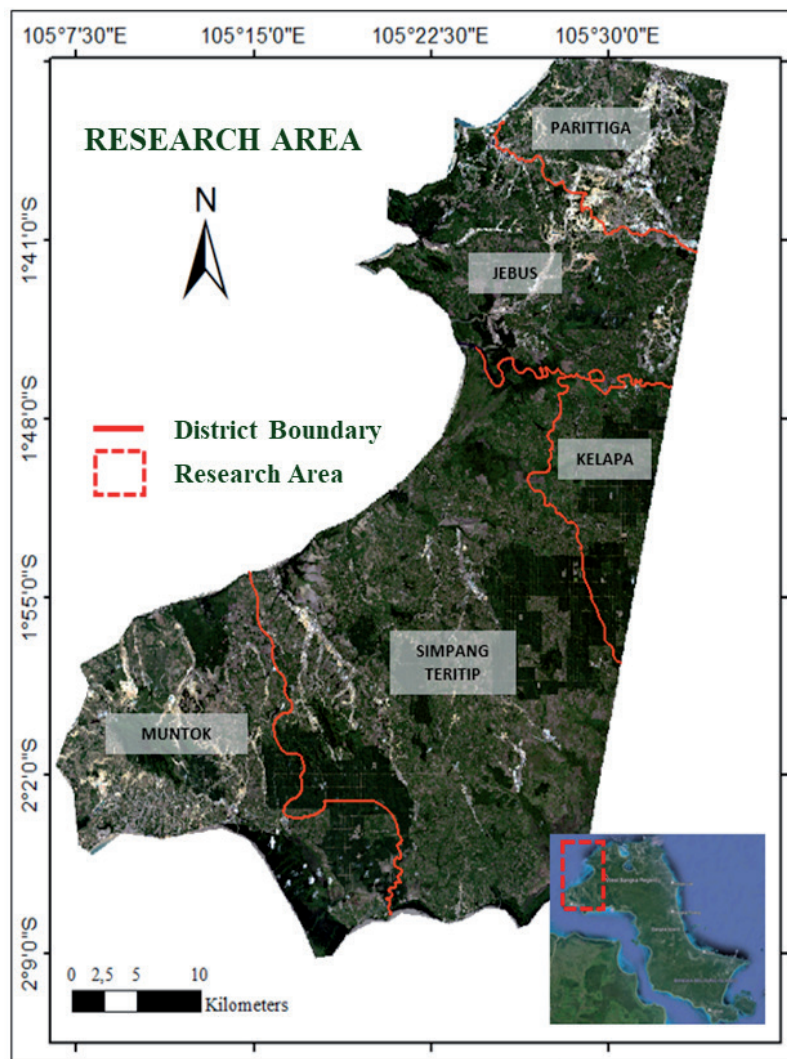


Figure 1. The research area in the north of Bangka Island is shown by a red-dotted polygon with a LANDSAT 8 image as a background.

Klabat granite is a source of tin mineralization and REE (Rare Earth Elements) through intensive and long-lasting erosion due to the leveling process on Bangka Island. The material was deposited and accumulated in paleochannel. This investigation, as the early detection methods of ancient grooves, is very important to localize prospect areas, especially in areas with limited access due to life safety factors, whether influenced by natural conditions, security, including health. During this pandemic, health issue is a very important factor that must be considered. Limited mobility makes geological surveys or direct observation activities in the field quite difficult because they require more costs and take longer time due to health protocols.

Based on these conditions, paleochannel investigations by this method for early detection, covering quite a large area and are simple enough to do and can be applied to tropical rainforest areas with dense vegetation and relatively low costs. In addition, this method was able to visualize the paleochannel traces in the study area that were not visible or detected in the optical image and DEMNAS data. It resulted in eleven traces, including four areas that were recommended to be followed up.

DATA AND METHODS

There are three images used in this study. LANDSAT 8 OLI (Operational Land Imager) images, DEMNAS data (National Digital Elevation Model), and radar images ALOS 2 PALSAR 2 (Advanced Land Observing Satellite 2 Phased Array type L-band Synthetic Aperture Radar 2). The use of these three images is based on the following thought pattern (Table 1):

Table 1. Characteristics of each image relevant to the investigation of paleochannel identification.

	LANDSAT-8	DEMNAS	ALOS 2 PALSAR 2
POSITIVES	<ul style="list-style-type: none"> Using optical sensors. It is effective for detecting open rivers and land cover. 	<ul style="list-style-type: none"> Combination of several radar images. They are able to penetrate vegetation and represent the measured elevation from the ground surface. 	<ul style="list-style-type: none"> Could penetrate to a certain depth depending on the wavelength and surface dielectric properties
NEGATIVES	<ul style="list-style-type: none"> Unable to penetrate vegetation and clouds. 	<ul style="list-style-type: none"> A model which is measured from the ground surface; there is no possibility to penetrate into the ground surface 	<ul style="list-style-type: none"> Required longer processing relatively

1. LANDSAT 8 optical sensors in the visible light wavelength range will capture both active and dry open river features.
2. DEMNAS data derived from several radar images produces elevation data measured from the ground surface, and it can capture enclosed river features not visible on the LANDSAT image, either covered by clouds or vegetation.
3. ALOS PALSAR 2 image using an L-Band frequency sensor ($\lambda = 23.6$ cm) can penetrate the clouds and vegetation cover and record the physical characteristics of the subsurface to a certain depth, depending on the dielectric properties of the covering material (Elachi and van Zyl, 2006; Saepuloh et al., 2015). The penetration ability of the layer increases as the surface is drier (Elachi & van Zyl, 2006). The SAR (Synthetic Aperture Radar) sensor with a wavelength in the L-channel range (23cm) is able to pass through cloud layers, volcanic gases, and canopy vegetation (Saepuloh, 2019). Therefore, L-channel SAR sensors are more effective for surface and near-surface detection than optical sensors. The effectiveness of the L-channel in detecting near-surface materials is shown in Figure 2, which shows the difference in surface recordings obtained from optical and SAR images. The bright, coarse texture of the SAR image comes from ancient coastal deposits with coarse fragments (Saepuloh, 2019). Based on this comparison, it is known that the SAR sensor allows it to detect materials near the surface, including paleochannel or rivers buried by alluvial.

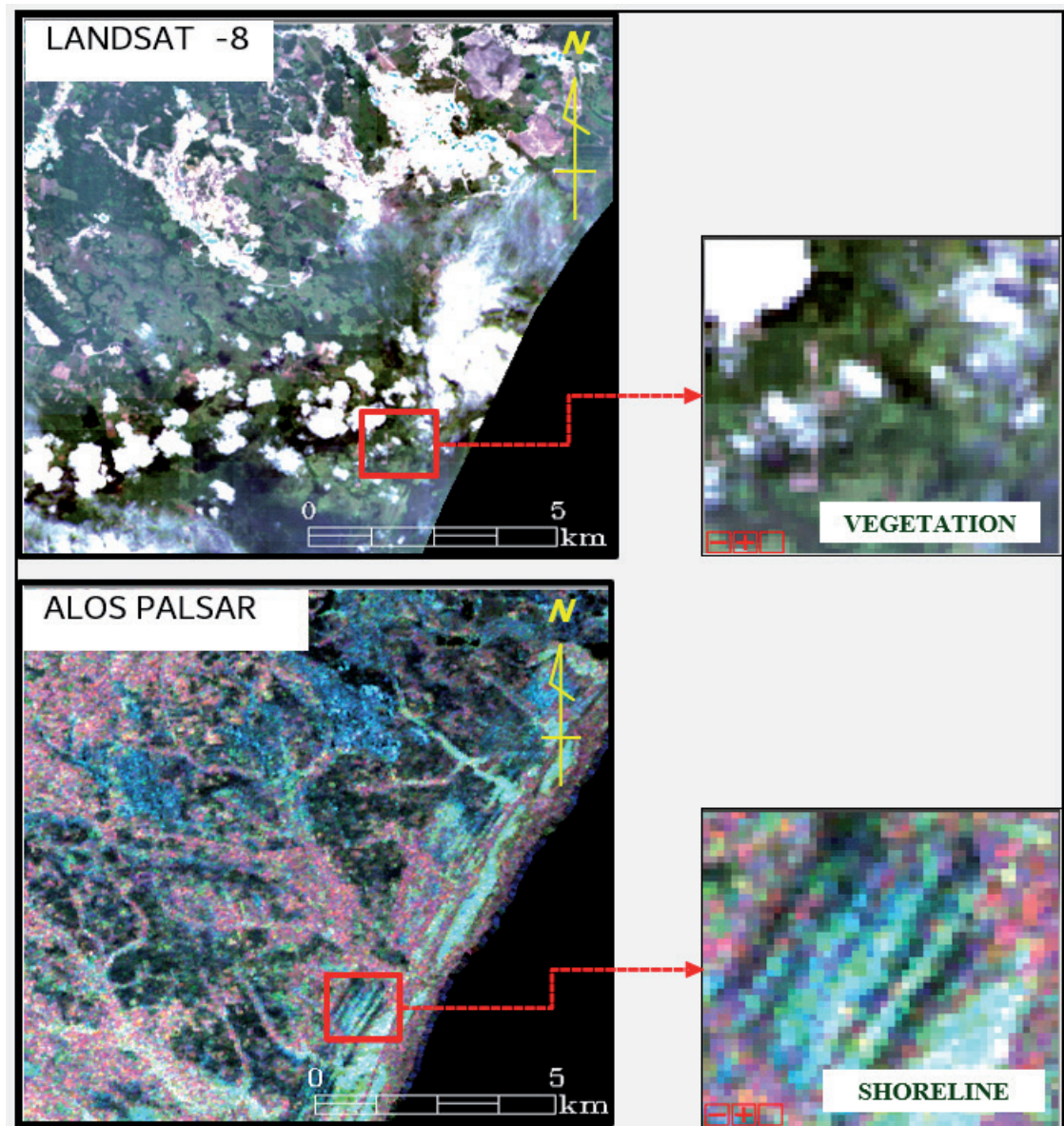


Figure 2. Illustration of the ancient shoreline detected by ALOS PALSAR image at the same location using LANDSAT 8 image only detected as vegetation cover in the southern part of Bangka Island (Saepuloh, 2019).

Detection of paleochannels has been applied qualitatively (visually) with a geomorphological approach. Each image is processed so that the contrasting features are clearly distinguishable visually, and this detection is carried out through three steps (see Figure 3).

1. Data Acquisition

This step includes data acquisition of ALOS 2 PALSAR 2 image, LANDSAT 8 image, and DEMNAS data. The LANDSAT 8 image selection is determined by considering the cloud cover level with the least cloud cover. While for ALOS 2 PALSAR 2, the selected image is the latest data in the JAXA archive (<https://auig2.jaxa.jp/>) and an image with acquisition time when the surface conditions tend to be dry regarded to rainfall and humidity in the research area. However, the research area is not covered by meteorological observation stations, so dry conditions are estimated based on the dry season months in Bangka Island. The images used each have specifications and characteristics, which can be seen in Table 2.

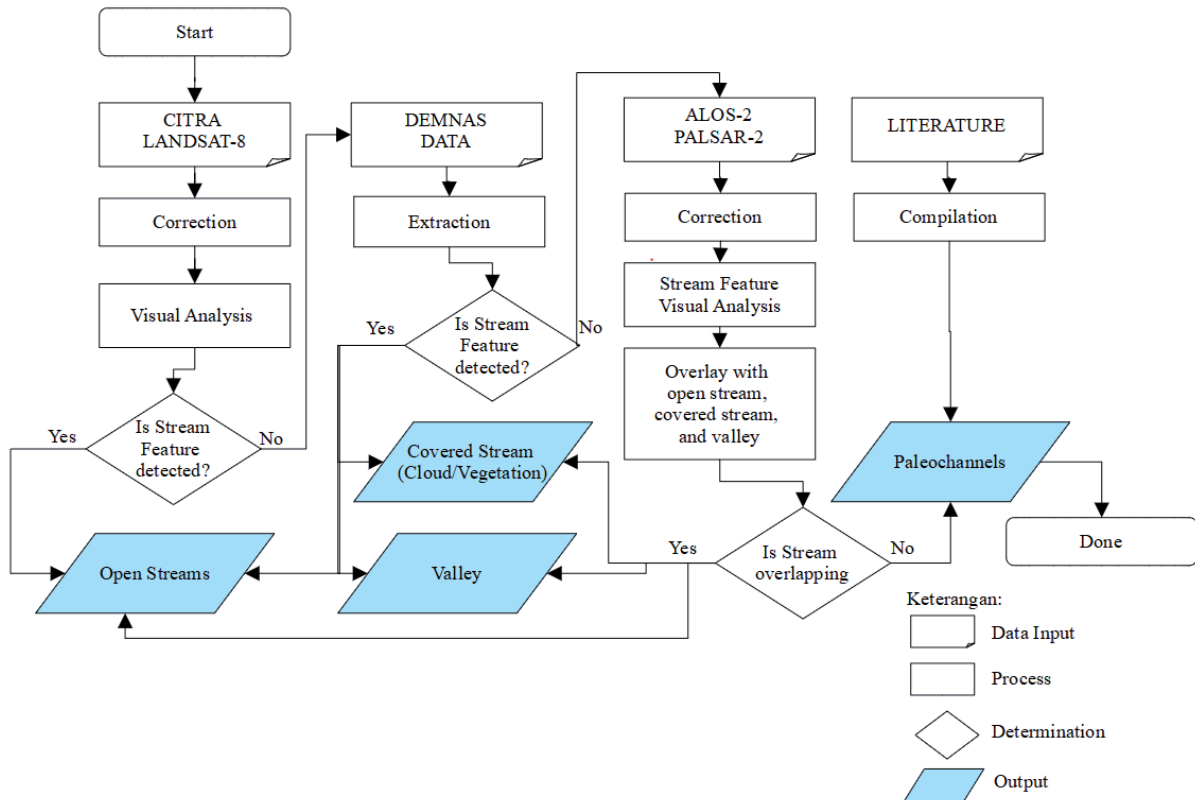


Figure 3. The research flow chart begins with the image data acquisition stage, visual analysis or extraction, overlaying river features from each image, and the result.

Table 2. Image specifications including ALOS 2 PALSAR 2 image, LANDSAT 8 OLI image, and DEMNAS data

No.	Scene ID	Acquisition Time	Remark
1.	ALOS2046957150-150406	April 6 th , 2015	<ul style="list-style-type: none"> • Level 1.1 • Ascending Orbit • Full Polarization • Resolution 12.5 m
2.	LC81240612015193LGN01	2015	<ul style="list-style-type: none"> • 9 bands • Sun-synchronous Orbit • Resolution 30 m
3.	DEMNAS_1114-14_v1.0 DEMNAS_1114-12_v1.0 DEMNAS_1114-11_v1.0 DEMNAS_1113-43_v1.0 DEMNAS_1113-44_v1.0	2018	<ul style="list-style-type: none"> • Combination of IFSAR, TERRASAR-X and ALOS 2 PALSAR 2. • Resolution 9 m

The ALOS 2 PALSAR 2 image was acquired on April 6th, 2015. Level 1.1 or SLC (Single Look Complex) with the coordinate system still in the slant range sensor coordinates. The processing was carried out by the CEOS (Committee on Earth Observation Satellites). The selected processing level was in the form of range compression, autofocus, and azimuth compression. The SLC data has the highest spatial resolution but the lowest focus. The ascending orbit shows the relative motion of the satellite from the south to the north pole of the earth with the direction of viewing the sensor to the east. Full Quad Polarization indicates that the image was acquired by utilizing the horizontal (H) - vertical (V) transmission and the horizontal-vertical incident wave with a full or complete combination of HH, HV, VH, and VV.

The LANDSAT 8 image was retrieved from <https://earthexplorer.usgs.gov/page>. This image was acquired in 2015 with an orbit close to the sun-synchronous circle or a nearly sun-synchronous polar orbit at an altitude of 705 km (Sitanggang, 2010). The LANDSAT 8 satellite has an OLI multispectral sensor (band 1-9) and a Thermal Infrared Sensor (band 10 and 11).

The DEMNAS data was downloaded from <https://tanahair.indonesia.go.id/demnas/#/page> for 5 scenes in GeoTIFF (TIF) format. This data was published by the Geospatial Information Agency in 2018 by integrating the IFSAR data (5 m resolution), TERRASAR-X (5 m resolution), and ALOS PALSAR (11.25m). The DEMNAS uses the 2008 EGM vertical datum with a spatial resolution of about 0.27 arc-second or 9 m. Although still in the development stage, this resolution is higher than the commonly used SRTM DEM data with a spatial resolution of about 1 arc-seconds or 30 m (Iswari & Anggraini, 2018)

2. Image processing of ALOS 2 PALSAR 2 and LANDSAT 8 OLI

Image processing of ALOS 2 PALSAR 2 consists of image correction and selection of composite images, and then visual detection is applied. The corrections consist of multilooking and geometric corrections. Multilooking is needed so that the morphology in the image can be seen visually, with high-quality focus and low speckle noise. However, the quality of the image focus is inversely proportional to the spatial resolution. The higher the image focus, the lower the spatial resolution obtained. The next correction is the geometric correction for adjusting the coordinates of the image (pixels) to the actual position on the earth's surface or according to the coordinates of a geographical map. By making geometric corrections, the image will be projected with a certain coordinate system so that it can be compared with other corrected images or spatial data.

In contrast to the processing of the ALOS 2 PALSAR 2 image, atmospheric correction is required for LANDSAT 8 optical image. This correction aims to reduce atmospheric effects so that more accurate earth surface conditions are obtained and increase the clarity or sharpness of the image so that the object under study can be observed (Saepuloh, 2019). These atmospheric effects cause refraction and reflection due to dust, fog, or smoke. Following the atmospheric correction, the LANDSAT 8 image the composed by RGB color composite for bands 4,3,2 to produce natural colors of the surface.

It's different from the radar and optical images; DEMNAS data does not require particular corrections. The data has been corrected, so the next step is just combining (mosaic) five images to obtain a complete image for extraction of the river stream. River stream delineation was performed by observing hydrological patterns and processing DEMNAS data in the form of filtering, including flow direction, flow accumulation, and stream order (Purwono et al., 2018).

3. Detecting the occurrence of paleochannels

The third step is image interpretation to identify the occurrence of paleochannels. Image interpretation is carried out visually based on the appearance or characteristics of the river channel that appears in the form of shape, object size, brightness level, pattern, texture, shadow, location or position and its association with surrounding objects. In the LANDSAT 8 image, the interpretation is carried out by the color composite image of RGB for bands 4,3,2, which could display the natural or actual color of objects on the earth's surface. The detected rivers stream from the natural color image is expected to be open rivers that appear to the LANDSAT 8 sensor without being covered or blocked by other objects. Contrary, the covered rivers are invisible to the LANDSAT 8 sensor. Therefore, the detection of covered rivers was carried out by simulated DEMNAS data. The river streams were defined by valleys flanked between ridges and indicated by a lower digital value than the surroundings so that visually it will appear relatively dark.

In radar images, the rougher the appearance of a surface, the higher the intensity of backscattering. Backscattering of objects in radar images is similar to reflectance in optical sensors, i.e., the ratio between the transmitted and returned wave power as a function of the object on the surface. This

backscattering value is quantified per area, referred to as the radar cross section (σ^0) with units of decibels (dB). The influenced parameters to the amount of backscattering could be grouped into two parts: the sensor system and the target or object on the surface. The parameters from the sensor system are the wavelength of the radar used (Band X, C, S, L and P), the type of polarization (HH, HV, VV, VH), depression angle or orientation, and resolution. The visual interpretation was performed by color composite R, G, B of backscattering intensity in ascending images for polarization types HH, HV, and VV.

RESULTS

Visualization of LANDSAT 8 image with natural color composite (R, G, B = band 4:3:2) was carried out to detect the appearance and color of the river in its actual condition, including the land cover of the surrounding area. There are three dominant colors for objects on land: dark green gradations, light green gradations, and brownish gray. Dark green gradations with regular boundaries are interpreted to be associated with the distribution of forests, oil palm plantations, and small hills. The light green color or gradation is associated with settlements and rice fields, while the gray-brown is associated with open areas, including mining areas.

The open rivers detected in the image are mostly main rivers which can be divided into two classes based on their color and texture. Dark blue color with a smooth texture indicates an open river that is still active and watery (Figure 4a). This appearance originated from the low water reflectance received by the sensor in the visible bands. On the contrary, dry rivers, as well as grey rivers due to sediment contamination, are presented as light brown with a rough texture.

The covered river streams by vegetation or other objects have been identified in DEMNAS data by utilizing the presence of river stream features in the valleys, but undetected by LANDSAT 8 imagery

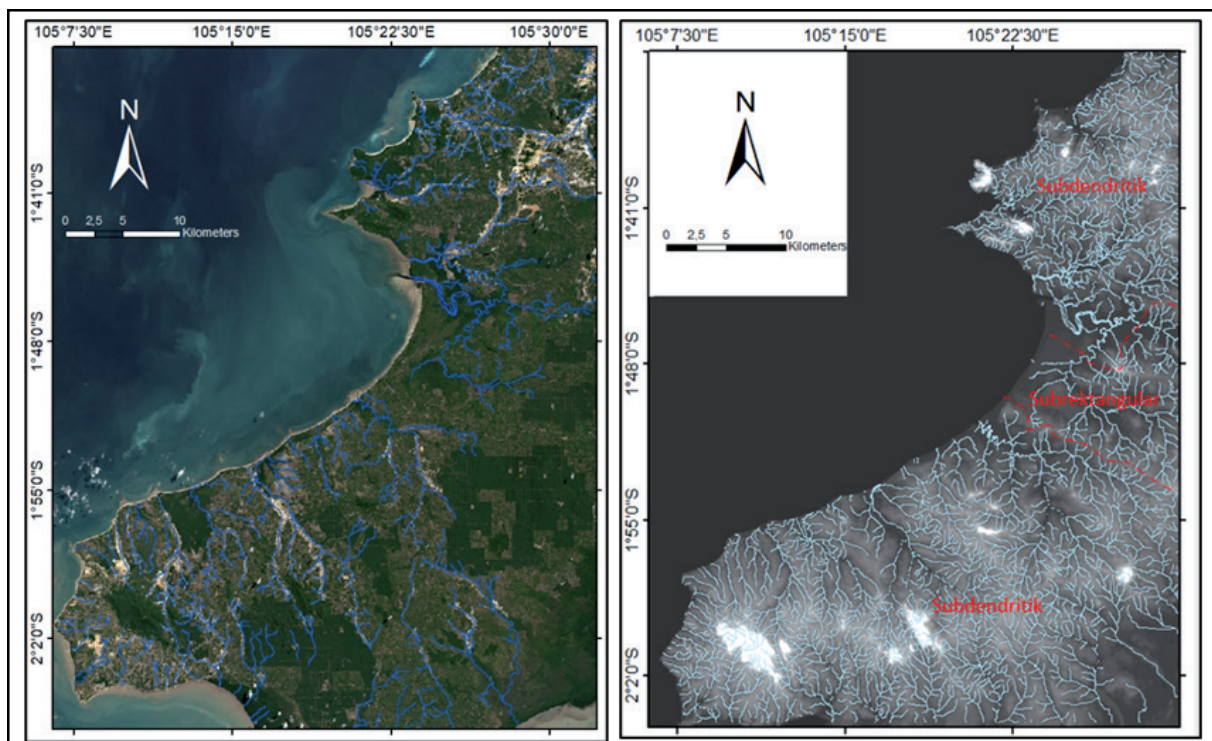


Figure 4. The open stream detected using the LANDSAT 8 image is shown by a blue polygon (a). Vegetation-covered rivers detected using DEMNAS data are marked with cyan polygons showing subdendritic and subrectangular stream patterns (b).

(Figure 4b). Therefore, it is possible that the identified streams from DEMNAS are more numerous than the actual rivers. Covered rivers identified using DEMNAS data are shadows of valleys flanked by slope morphology between hills. The low elevation in DEMNAS but high contrast topography with the surroundings reflects the presence of the river streams.

The small river streams or tributaries have been well identified by DEMNAS. According to visual detection, the study area is dominated by a subdendritic pattern and a subrectangular in the middle with developed meander morphology. This condition indicates that the study area tends to have a sloping morphology with long erosion. The subdendritic pattern is slightly different from the dendritic pattern due to the influence of the geological structure or topographic pattern (Howard, 1967).

Eleven locations were identified as paleochannels based on the visualization of the color composite image of the ALOS 2 PALSAR 2 (Figure 5). The image visualization shows five dominant colors, i.e., green, pink, bluish-purple, black, and, in some places, bright white to pink. The green indicates a relatively medium to rough surface texture. The bright color indicates the rough surface, interpreted as the presence of sand-sized material (Saepuloh, 2019). The bluish-purple is associated with open mining

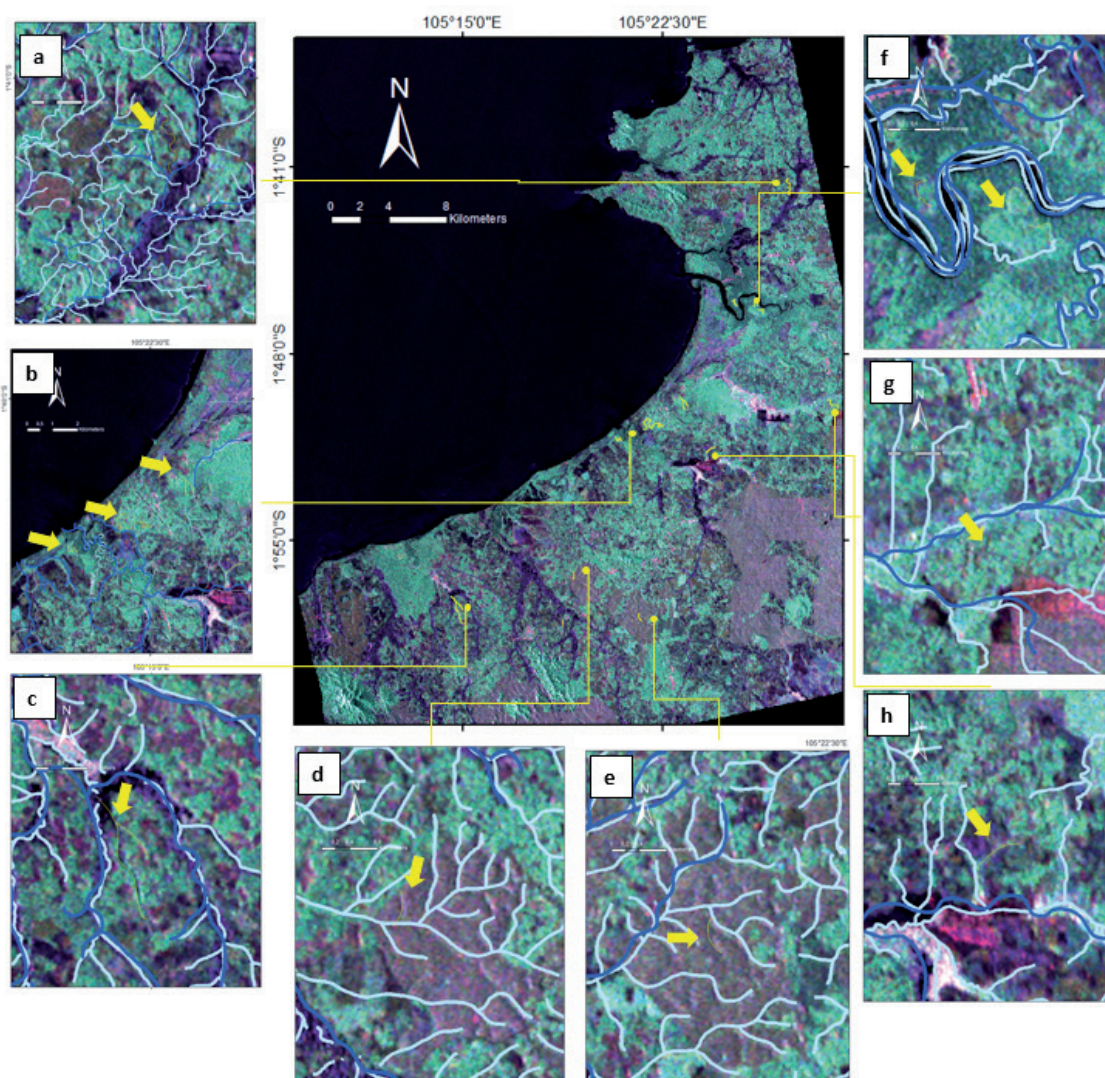


Figure 5. Eleven paleochannel locations in the study area. Three points adjacent to the mine opening area (a, c and h), three points adjacent to the coast (b), three points associated with the upstream of the covered river by vegetation (d-e, g), and two points adjacent to the river meander are indicated by dark blue and light blue polygons that intersect to form curves (f).

(Susanto, 2015). Dark purple indicates the domination of fine materials, ranging in size from clay to silt (Saepuloh, 2019). The dark smooth texture came from a flat surfaces such as active river streams and watered meanders. This zone is mostly located near the coast forming a river meander morphology. A bright red with a rough texture indicates a relatively rough surface, interpreted as gravel or even lump-sized material. When compared with the LANDSAT 8 image, the area is dominated by a rough texture identical to the plantation (Susanto, 2015). We suggested that the volume scattering of dense tree trunks and rock fragments under the canopy causes a coarse texture in the ALOS 2 PALSAR 2 image.

The traces of paleochannels recorded in the ALOS 2 PALSAR 2 composite image are associated with meandering rivers, small rivers, near the coast, and close to mining areas. In general, paleochannels associated with meander rivers are located in the position of a buried point bar or oxbow lake (Figure 5f). In the river's upper reaches, it appears as a river branch but is not detected by LANDSAT 8 and DEMNAS images and is generally covered by dense vegetation (Figures 5d-e and 5g). In addition, there is also a paleochannel close to the coast in the form of faint grooves (5b). Finally, paleochannels around the mine openings are shown in bluish-purple (6a-c and 6h).

DISCUSSION

Visual identification of paleochannels in the study area is quite challenging due to the existence of the open mining area parallel to the current active rivers. Overcoming the problem, we examined the river stream pattern detail using the LANDSAT 8 optical image. According to the color composite of ALOS 2 PALSAR 2 for R, G, B = HH, HV, VV, the existence of paleochannels is presented by the purple to dark or bright, green, and pink zones. Its presence is generally adjacent to river meanders, beaches, or small channels.

The detected paleochannels based on morphology were located randomly with discontinuity stream patterns due to the limited penetration of the ALOS 2 PALSAR 2 sensor. The relatively high humidity around the study area, about 74% to 88%, resulted in the variation of the detected river streams. Interpretation and verification of paleochannels continuity could be performed by field investigation, such as detailed geological observation, drilling, and geophysical surveys.

As part of the verification process, we utilized field data in the form of mining following the river streams. Tin mining soil contains quartz as a residue from weathering of granite. In addition, the miner's opening zone is generally in the form of holes filled with water, commonly called "Kolong". The dimensions of the pit determine the scale of the tin mining operation. The open mining area from 1989 to 2014 shows an increasingly widespread change (Susanto, 2015). In 1989, open mining areas were identified as narrow areas in the north and south of Bangka and continued to expand to the central part of West Bangka Regency.

According to the detected paleochannels with mining locations, most of the identified paleochannels in the ALOS 2 PALSAR 2 image are in the mining area and under the mine. This agreement is used to verify the existence of paleochannels, considering the location of alluvial or placer mines is closely associated with tin placer deposits formed in ancient grooves. The identification of these paleochannels was also verified by the results of PT Timah's onshore exploration drilling, which correlated with the presence of a paleochannel in the purple zones of the ALOS 2 PALSAR 2 image (Figure 6). In addition to tin, the identification of this ancient groove is very interesting, especially regarding the potential for other mineral deposits still associated with cassiterite, such as monazite, as a carrier of rare earth metals or radioactive elements such as thorium and uranium. These potentials are closely correlated with granite batholiths as mineralization carriers exposed in the study area (Figure 6).

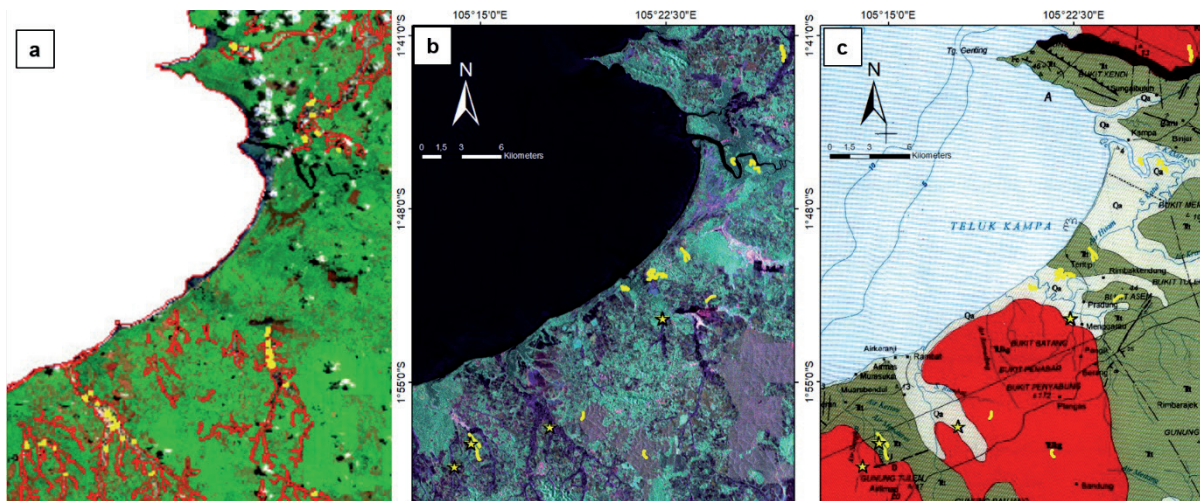


Figure 6. Comparison of the location of the open mining area marked with red polygons and the pits marked with yellow polygons (a). The detected ancient grooves marked with yellow polygons (b) and yellow stars are onshore exploration drilling points of PT Timah Tbk's. The position of the ancient groove in the geological map is in the distribution of Klabat Granite as a carrier of mineralization (Mangga & Djamal, 1994), which is shown by a yellow polygon and the prospect area for further analysis is indicated by a dotted yellow circle (c).

CONCLUSIONS

Channel features were detected very well using ALOS 2 PALSAR 2 radar image but not detected in LANDSAT 8 image as an open river or DEMNAS as a covered river. The appearance of these river channels is identified as paleochannels. The paleochannels detected from the ALOS 2 PALSAR 2 SAR image are scattered randomly in the form of separate and discontinuous river stream patterns. The position of the paleochannels has been covered by old mining areas, plantations, farmlands, and forests.

The identification of this paleochannel is supported by previous literature data in the form of the distribution of old mining and underground areas, which are closely correlated with the exploitation of secondary tin deposits in the form of placers. This condition is also closely correlated with the presence of paleochannels. In addition, the distribution of PT Timah's onshore exploration drilling points, which proves the existence of a paleochannel in the research area, also intersects with purplish-colored zones near the mine area. This fact further strengthens that the purple-graded areas in the ALOS 2 PALSAR 2 image are closely related to the presence of paleochannels in the study area.

Prospect areas for the existence of paleochannel are closely correlated with the presence of granite batholiths, both from proximity and from the interpretation of the possibility of paleochannel upstream associated with granitic batholiths. The next step of this study is geophysical surveys, detailed geological mapping, or shallow drilling. Field observation activities have also become effective and efficient because the targets have been very well-defined in advance. On the other hand, the field survey results validated the image interpretation. This study supports exploration activities in Indonesia, particularly in delineating placer areas remotely.

REFERENCES

- Bennett, G. L., Weissmann, G. S., Baker, G. S., & Hyndman, D. W. (2006). Regional-scale assessment of a sequence-bounding paleosol on fluvial fans using ground-penetrating radar, eastern San Joaquin Valley, California. *Geological Society of America Bulletin*, 118, 724–732.
- Cobbing, E. J., Mallick, D. I. J., Pitfield, P. E. J., & Teoh, L. H. (1986). The granites of the southeast Asian tin belt. *Journal of the Geological Society*. <https://doi.org/10.1144/gsjgs.143.3.0537>
- Elachi, C., & van Zyl, J. (2006). Introduction to the Physics and Techniques of Remote Sensing: Second Edition. In *Introduction to the Physics and Techniques of Remote Sensing: Second Edition*. <https://doi.org/10.1002/0471783390>
- Howard, A. D. (1967). Drainage Analysis in Geologic Interpretation: A Summation. *The American Association of Petroleum Geologist Bulletin*, 51, 2246–2259. <https://doi.org/10.1306/5d25c26d-16c1-11d7-8645000102c1865d>
- Iswari, M. Y., & Anggraini, K. (2018). Demnas: Model Digital Ketinggian Nasional untuk Aplikasi Kepesisiran. *OSEANA, XLIII*, 68–80. <https://doi.org/10.14203/oseana.2018.vol.43no.4.2>
- Kottek, M., Grieser, J., Beck, C., Rudolf, B., & Rubel, F. (2006). World map of the Köppen-Geiger climate classification updated. *Meteorologische Zeitschrift*. <https://doi.org/10.1127/0941-2948/2006/0130>
- Mangga, S. A., & Djamal, B. (1994). *Peta Geologi Lembar Bangka Utara, Sumatera*. Pusat Penelitian dan Pengembangan Geologi.
- Paillou, P., Tooth, S., & Lopez, S. (2012). The Kufrah paleodrainage system in Libya: A past connection to the Mediterranean Sea? *Comptes Rendus - Geoscience*. <https://doi.org/10.1016/j.crte.2012.07.002>
- Purwono, N., Hartanto, P., Prihanto, Y., & Kardono, P. (2018). Teknik Filtering Model Elevasi Digital (Dem) Untuk Delineasi Batas Daerah Aliran Sungai (Das). *Seminar Nasional Geografi UMS IX 2018, Restorasi Sungai: Tantangan dan Solusi Pembangunan Berkelanjutan*, 490–504.
- Saepuloh, A. (2019). *Prinsip dan Aplikasi Penginderaan Jauh Geologi Gunung Api* (Edisi 1). ITB Press.
- Saepuloh, A., Koike, K., Urai, M., & Sumantyo, J. T. S. (2015). Identifying surface materials on an active volcano by deriving dielectric permittivity from polarimetric SAR data. *IEEE Geoscience and Remote Sensing Letters*, 12(8), 1620–1624. <https://doi.org/10.1109/LGRS.2015.2415871>
- Sitanggang, G. (2010). Kajian Pemanfaatan Satelit Masa Depan : Sistem Penginderaan Jauh Satelit LDCM (Landsat-8). *Berita Dirgantara*, 11, 47–58.
- Susanto. (2015). Daerah Kolong Timah di Bangka Belitung dengan Data Satelit SPOT 6. *Seminar Nasional Sains dan Teknologi 2015 Fakultas Teknik Universitas Muhammadiyah Jakarta*.
- Zainal, M., Yanis, M., Muksin, U., & Ismail, N. (2017). Investigasi Sungai Purba Berdasarkan Metode Electrical Resistivity Tomography di Banda Aceh. *Journal of Aceh Physics Society*, 6, 1–5.
- Zhang, S., Ma, Y., Chen, F., Liu, J., Chen, F., Lu, S., Jiang, L., & Li, D. (2020). A new method for supporting interpretation of paleochannels in a large scale — Detrended Digital Elevation Model Interpretation. *Geomorphology*. <https://doi.org/10.1016/j.geomorph.2020.107374>